

A LINEARIZED ANALYSIS & DESIGN
OF AN AUTOMATIC BALANCING
SYSTEM FOR THE THREE AXIS

AIR BEARING TABLE

by
Felix Zajac & David Small

I-622-63-81

Stabilization & Control Branch
Spacecraft Systems & Projects Division
Goddard Space Flight Center
April 25, 1963

Reviewed: C. Cantor
C. Cantor, Head
System Development Section
Stabilization & Control Branch

Approved: H. C. Hoffman
H. C. Hoffman, Head
Stabilization & Control Branch

TABLE OF CONTENTS

	Page
LIST OF FIGURES 3
INTRODUCTION 4
DEFINITIONS 5
ANALYSIS	
Table Dynamics 8
Control Systems 12
COMPUTER RESULTS	
Roll Axis (Roll-yaw balancing mode) 14
Yaw Axis (Either balancing mode) 14
Roll Axis (Pitch balancing mode) 14
INTER-AXIS CROSS-COUPLING 15
CONCLUSION 17
APPENDIX 18

LIST OF FIGURES
(Figures at end of report)

FIGURE

- I DIAGRAM OF ROLL-YAW BALANCING MODE
- II DIAGRAM OF PITCH BALANCING MODE
- III SERVO BLOCK DIAGRAM OF THE BALANCING SYSTEM
- IV BODE PLOT - ROLL AXIS CONTROL
- V BODE PLOT - YAW AXIS CONTROL
- VI TYPICAL ROLL RESPONSE - UNBALANCE TORQUE VERSUS TIME
- VII CHART OF INITIAL UNBALANCE TORQUE VERSUS SETTLING TIME TO 5000
 DYNE-CM BALANCE FOR THE ROLL AXIS CONTROL
- VIII TYPICAL YAW RESPONSE - UNBALANCE TORQUE VERSUS TIME
- IX CHART OF INITIAL UNBALANCE TORQUE VERSUS SETTLING TIME TO 5000
 DYNE-CM BALANCE FOR THE YAW AXIS CONTROL
- X ANALOG DIAGRAM OF THE BALANCING SYSTEM

INTRODUCTION

For the air bearing table to achieve its purpose of testing satellite attitude control systems, the extraneous torques on the table must be eliminated, if not totally, then to a value that will not affect the function of the attitude control system. When the design of the present attitude control system for the table was simulated on the analog computer, extraneous torques up to 10,000 dyne-cms. around each axis were simulated with no apparent affect on the performance of the attitude control system. Most attitude control systems for satellites do not require a finer torquing control than that in the present table control system. Hence, elimination of extraneous (unbalanced) torques to within 10,000 dyne-cms. is sufficient, not only for the present table control system, but for most attitude control systems that will be tested on this table in the future.

Of the many causes of unbalanced torques (temperature changes, air currents, static mass unbalance, magnetic fields, etc.), static mass unbalance contributes substantially to the total unbalance. This report presents the analysis and design of an automatic control system to reduce this mass unbalance to 5000 dyne-cms. or less.

To balance the table (eliminate the static mass unbalance) about three axes, the table is first balanced manually to within 200,000 dyne-cms. of torque balance in the horizontal position. After this balancing the table should be pendulous, but with a period greater than 2.0 minutes. The table is then released from an appropriate initial position, and the automatic balancing system is activated. This system senses a positional error from the initial position, resulting from a torque unbalance, and corrects this unbalance by driving a weight along the appropriate axis.

Two different initial positions (balancing modes) of the table are needed to balance the table in three axes. In position one (FIGURE I), the balancing system is in operation in the roll and yaw axes. Consequently, after the table is balanced in these axes, the center of gravity (c.g.) will lie on the pitch axis. In position two (FIGURE II), the table is rotated through 20 degrees about the roll axis, where the pitch balancing mode is initiated and the movement of the pitch weight (W_p) brings the c.g. to coincide with the center of rotation (C.R.), completing the table balancing about all three axes. In the pitch balancing mode, an additional position sensor is used together with the yaw balancing controls to limit table movement relative to the axis "Y". Finally, the table should be returned to the first position and the balancing procedure repeated in the roll and yaw axes. The following is the analysis and design of the complete balancing system.

DEFINITIONS

θ_R, θ_Y	- angular position of table about the roll and yaw axes, respectively.	...radians
ω_R, ω_Y	- angular velocity of table about the roll and yaw axes, respectively.	...radians/sec
d	- dead zone of d.c. servomotor	...d.c. volts
L	- saturation voltage of d.c. servomotor	...d.c. volts
K_M	- gain of d.c. servomotor	...rad/sec/d.c. volt
T_M	- time constant of d.c. servomotor	...seconds
n	- gear reduction	...rad/rad
K_L	- lead screw reduction	...ft/rad
W_T	- weight of table	...lbs
R_R, R_Y	- the perpendicular distance from the center of gravity (c.g.) to the roll and yaw axes (FIGURE I)	...ft
R_P	- the distance from the c.g. to the center of rotation (C.R.) (FIGURE II)	...ft
ϕ_R	- angle formed by the intersection of the line from the c.g. to the roll axis (R_R) and the roll-pitch plane (FIGURE I)	...rad
ϕ_Y	- angle formed by the intersection of the line from the c.g. to the yaw axis (R_Y) and the yaw-pitch plane (FIGURE I)	...rad
ϕ_P	- initial angular position of table about the roll axis when the pitch balancing mode is used (FIGURE II).	...rad
K_{SR}, K_{SP}	- gain of position sensor in the roll axis control in the roll-yaw and pitch balancing modes, respectively	...a.c. volts/rad
K_{SY}	- gain of position sensor in the yaw axis control in both balancing modes	...a.c. volts/rad

K_{DR}, K_{DP}	- gain of demodulator in the roll axis control in the roll-yaw and pitch balancing modes, respectively	...d.c. volts/ a.c. volts
K_{DY}	- gain of demodulator in the yaw axis control in both balancing modes	...d.c. volts/ a.c. volts
τ_{IR}, τ_{IP}	- lead time constants of lead-lag networks in the roll axis control in the roll-yaw and pitch balancing modes, respectively	...seconds
τ_{IY}	- lead time constant of lead-lag network in the yaw axis control in both balancing modes	...seconds
τ_{2R}, τ_{2P}	- lag time constants of lead-lag networks in the roll axis control in the roll-yaw and pitch balancing modes, respectively	...seconds
τ_{2Y}	- lag time constant of lead-lag networks in the yaw axis control in both balancing modes	...seconds
τ_{3R}, τ_{3P}	- time constants of filter networks in the roll axis control in the roll-yaw and pitch balancing modes, respectively	...seconds
τ_{3Y}	- time constant of filter networks in the yaw axis control in both balancing modes	...seconds
K_{AR}, K_{AP}	- gain of amplifier in the roll axis control in the roll-yaw and pitch balancing modes, respectively	...d.c. volts/ d.c. volts
K_{AY}	- gain of amplifier in the yaw axis control in both balancing modes	...d.c. volts/ d.c.volts
r_R, r_P	- position of control weight in the roll axis control in the roll-yaw and pitch balancing modes, respectively	...ft
r_Y	- position of control weight in the yaw axis control in both balancing modes	...ft
w_R, w_P	- control weight in the roll axis control in the roll-yaw and pitch balancing modes, respectively	...lbs

W_Y	- control weight in the yaw axis control in both balancing modes	...lbs
I_{RR}, I_{YY}, I_{PP}	- moment of inertia of table about the roll, yaw, and pitch axes, respectively. $I_{RR} = 50 \text{ slug-ft}^2$, $I_{YY} = 27 \text{ slug-ft}^2$, $I_{PP} = 50 \text{ slug-ft}^2$	
T_{WR}, T_{WP}	- torque about roll axis due to moving weight when the balancing system operates in the roll-yaw and pitch balancing modes, respectively	...ft-lbs
T_{WY}	- torque about yaw axis due to moving weight when the balancing system operates in both balancing modes	...ft-lbs
T'_{UR}, T'_{UP}	- torque about roll axis due to initial static mass unbalance when balancing system operates in the roll-yaw and pitch balancing modes, respectively	...ft-lbs
T'_{UY}	- torque about yaw axis due to initial static mass unbalance when balancing system operates in both balancing modes	...ft-lbs
T_{PR}, T_{PY}	- incremental torque about roll and yaw axes, respectively, due to c.g. below the roll-yaw plane (pendulosity).	...ft-lbs
T_{UR}, T_{UY}	- total torque unbalance around the roll and yaw axes, respectively	...ft-lbs

ANALYSIS

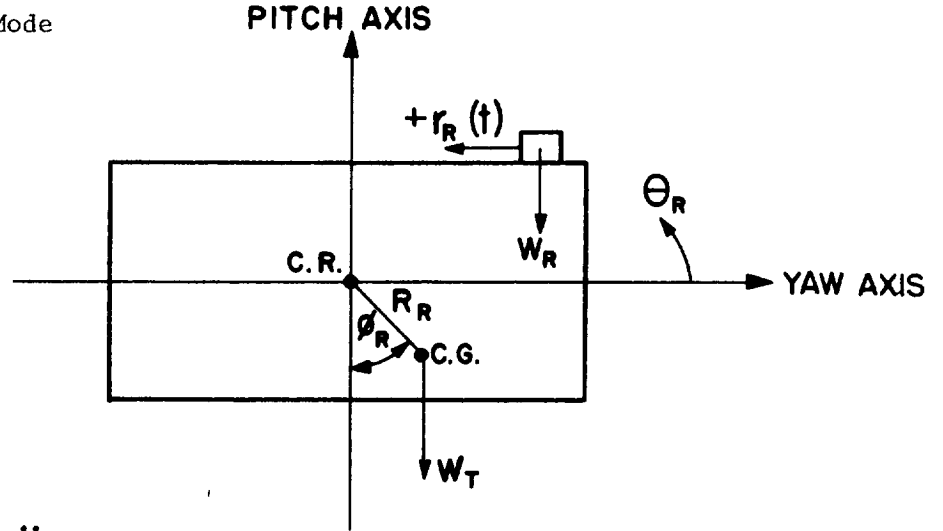
Table Dynamics

Before the balancing system can be analyzed and designed, the table dynamics about each axis must be determined. The table dynamics about the roll and yaw axes, corresponding to position I (FIGURE I), will be analyzed first. Afterwards, the dynamics in the pitch balancing mode (FIGURE II) will be determined.

Position 1

Roll-Yaw Balancing Mode

Roll Axis



$$(1) \sum T_R = I_{RR} \ddot{\theta}_R$$

(This is a linear approximation of the general equations of angular motion of a rigid body. Its validity will be shown later in this report.)

$$(2) \sum T_R = W_R r_R(t) \cos \theta_R - W_T R_R \sin(\phi_R + \theta_R) = I_{RR} \ddot{\theta}_R$$

$$(3) \sin(\phi_R + \theta_R) = \sin \phi_R \cos \theta_R + \sin \theta_R \cos \phi_R$$

for small variations of θ_R :

Hence:

$$\sin(\phi_R + \theta_R) = \sin \phi_R + \theta_R \cos \phi_R \quad \text{since } \cos \theta_R = 1$$

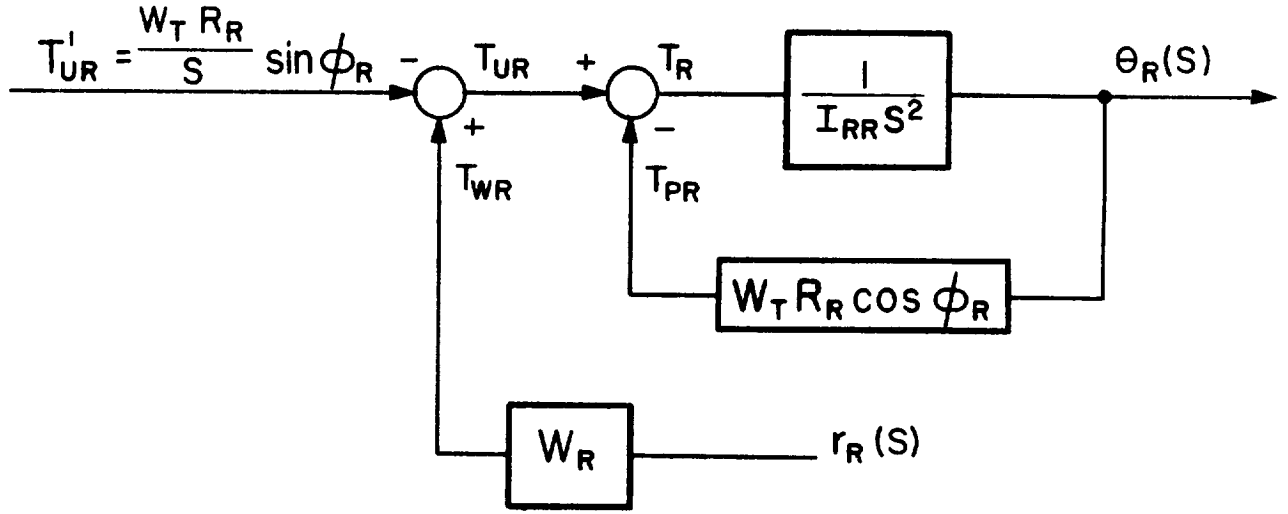
$$(4) W_R r_R(t) - W_T R_R \sin \phi_R - W_T R_R \theta_R \cos \phi_R = I_{RR} \ddot{\theta}_R$$

With all initial conditions zero, the LaPlace transform yields:

$$(5) W_R r_R(s) - \frac{W_T R_R}{s} \sin \phi_R = [I_{RR} s^2 + W_T R_R \cos \phi_R] \theta_R(s)$$

$$\text{or (6) } \theta_R(S) = \frac{1}{I_{RR} S^2 + W_T R_R \cos \phi_R} \left[W_R r_R(S) - \frac{W_T R_R}{S} \sin \phi_R \right]$$

The corresponding servo block diagram is shown below:



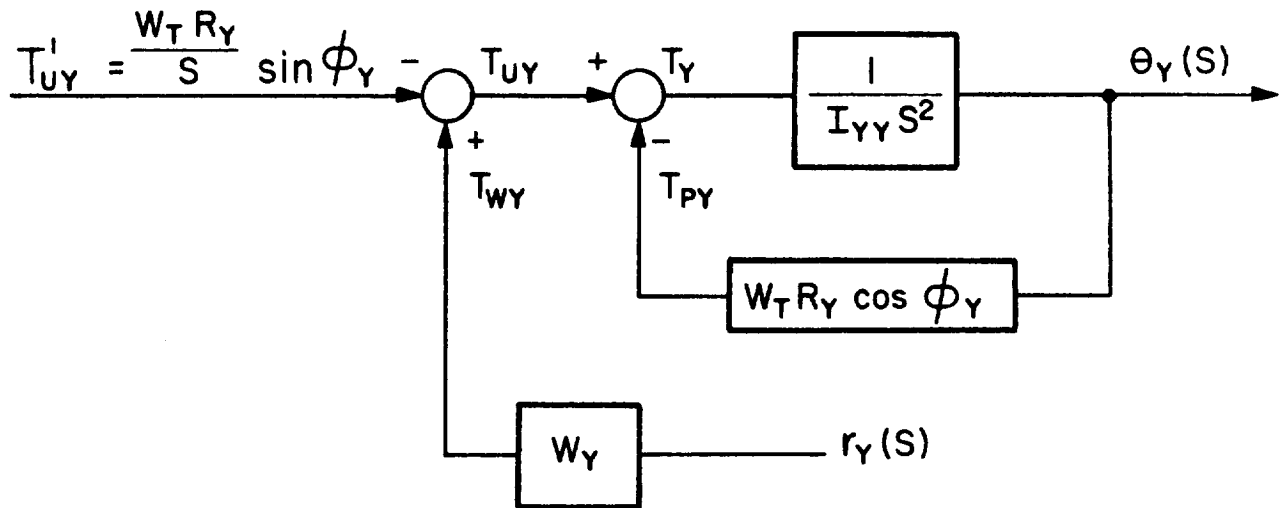
Of course, this block diagram will appear as part of the overall roll axis control loop, in the roll-yaw balancing mode.

Yaw Axis

The dynamics for the yaw axis can be obtained in the same manner, giving:

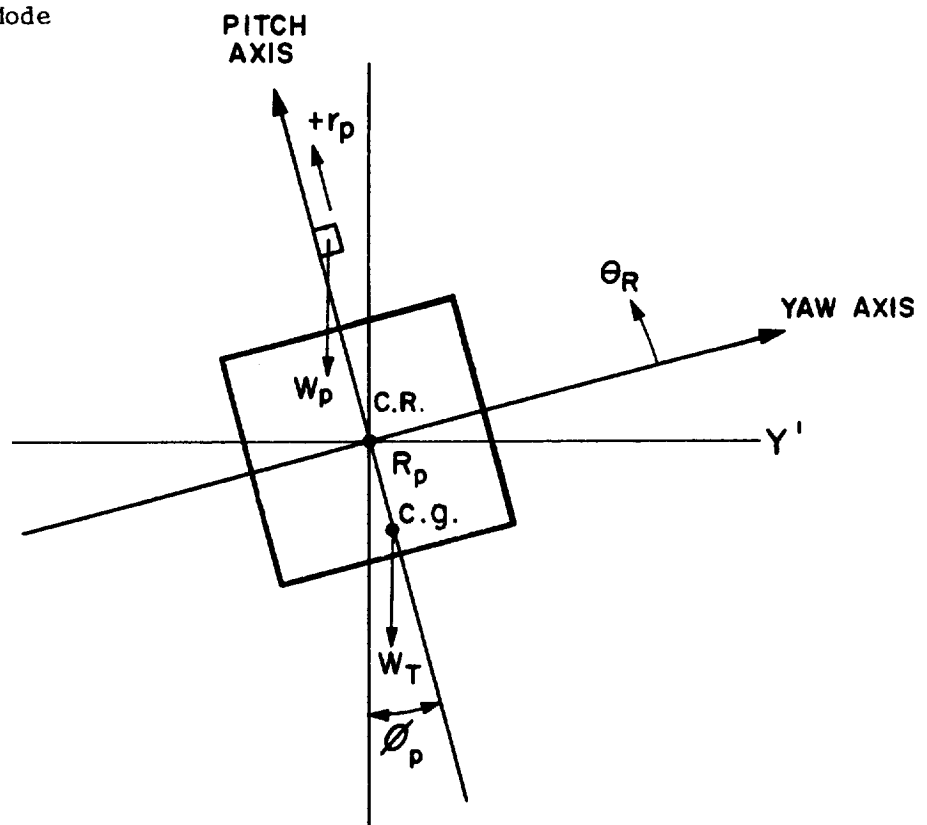
$$(7) \theta_Y(S) = \frac{1}{I_{YY} S^2 + W_T R_Y \cos \phi_Y} \left[W_Y r_Y(S) - \frac{W_T R_Y}{S} \sin \phi_Y \right]$$

The corresponding servo block diagram for the yaw axis dynamics is shown below. This will form part of the overall yaw axis control loop, in the roll-yaw balancing mode.



Position 2
Pitch Balancing Mode

Roll Axis



Note: All roll angles and torques are positive in the counterclockwise direction.

$$(8) \quad \Sigma T_R = I_{RR} \ddot{\theta}_R$$

$$(9) \quad W_P r_P \sin(\phi_P + \theta_R) - W_T R_P \sin(\phi_P + \theta_R) = I_{RR} \ddot{\theta}_R$$

$$(10) \quad \sin(\phi_P + \theta_R) = \sin \phi_P \cos \theta_R + \cos \phi_P \sin \theta_R$$

for small variations of θ_R :

$$(11) \quad \sin(\phi_P + \theta_R) = \sin \phi_P + \cos \phi_P (\theta_R)$$

Hence:

$$(12) \quad W_P r_P [\sin \phi_P + (\cos \phi_P) \theta_R] - W_T R_P [\sin \phi_P + (\cos \phi_P) \theta_R] = I_{RR} \ddot{\theta}_R$$

$$\text{Since } \phi_P \gg \theta_R, \sin \phi_P \gg (\cos \phi_P) \theta_R$$

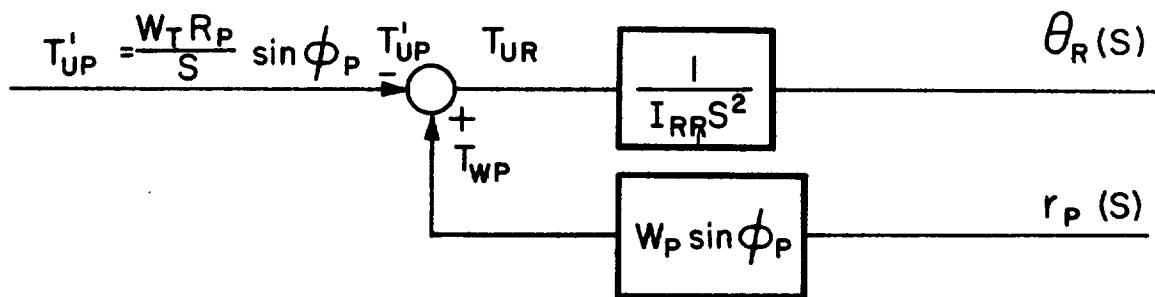
Therefore equation (11) reduces to

$$(13) \quad W_P r_P [\sin \phi_P] - W_T R_P [\sin \phi_P] = I_{RR} \ddot{\theta}_R$$

With all initial conditions zero, the LaPlace transform yields:

$$(14) \quad W_P r_P (S) \sin \phi_P - \frac{W_T R_P}{S} \sin \phi_P = [I_{RR} S^2] \theta_R (S)$$

$$\text{or (15) } \theta_R (S) = \frac{1}{I_{RR} S^2} [W_P (\sin \phi_P) r_P (S) - \frac{W_T R_P}{S} \sin \phi_P]$$



With the table dynamics linearized, a linear analysis and design of the balancing system can now be effected.

CONTROL SYSTEMS

Roll Axis Control (Roll-Yaw Balancing Mode)

The block diagram of this system is shown in FIGURE III. An explanation of the system and each component is described below.

The torque unbalance (T_{UR}') of the table causes a table position error (θ_R). The position sensor is an electrolytic potentiometer. When used in an a-c bridge circuit, it gives a proportional a-c signal up to $\pm 3/4$ degrees of table tilt. The electronic demodulator produces a d-c signal whose polarity depends upon the phase of the a-c signal (i.e., the direction of tilt of the table). Due to excessive lag and instability, two lead-lag compensating networks are used to produce the necessary compensation. Any high frequency noise is attenuated via filter networks. (It is possible to utilize the motor armature inertia to obtain a lead effect. However the amount of this lead would be too small for the present system. See Appendix)

Since the motor has a dead zone of ± 2 volts, an amplifier of gain ten is added so that in a steady-state condition the tilt of the table will be within $\pm 1\frac{1}{2}$ minutes of arc, the resolution of the sensor. Moreover, a limiting device set at ± 30 volts is used to protect the motor. The d-c motor with its gear reducer drives the control weight producing a compensatory torque (T_{WR}) on the table.

A Bode diagram of the uncompensated system ($G_{(UNC)R}(S)$) for $\phi_R = 90^\circ$ (non-pendulous condition, which is the worst case) is plotted in FIGURE IV. The compensating networks were designed to give system unity gain crossover at 0.5 rad/sec., and 52 degrees of phase margin. The time constants of the lead-lag networks are chosen to be $T_{1R} = 10$ seconds, and $T_{2R} = 0.333$ seconds while the time constant of the noise filters is set at 0.0333 seconds. The corresponding Bode diagram of the compensated system ($G_{(C)R}(S)$) is also shown in FIGURE IV. Notice that the gain may fluctuate as much as ± 14 db (a factor of 5 to a factor of 0.2) before the system goes unstable (i.e., the gain margins are ± 14 db).

Yaw Axis Control (Both Balancing Modes)

The block diagram of this system is shown in FIGURE III. Due to the similarity of this control system to the roll control system, a detailed explanation will not be made.

Since the moment of inertia of the yaw axis differs from the moment of inertia of the roll axis, the time constants of the lead-lag networks assume new values for near optimum response. These are $T_{1Y} = 7.13$ seconds and $T_{2Y} = 0.25$ seconds. The control weight is increased by a factor of two, increasing the gain by two. The Bode diagrams of the uncompensated and

compensated systems for $\phi_y = 90$ degrees are shown in FIGURE V. The resulting 0 db frequency crossover for the compensated system is 1.0 rad/sec and the phase margin is 48 degrees. The corresponding gain margins are +12 db and - 18 db (a factor of 3.9 to a factor of 0.12).

Roll Axis Control (Pitch Balancing Mode)

The block diagram of this system is shown in FIGURE III. The only difference between this system and the roll control system in the roll-yaw balancing mode is the gain from the control weight to the torque on the table produced by this weight. In the roll-yaw balancing mode this gain is $W_R r_R(t)$ as compared to a gain in the pitch balancing mode of $W_p r_p(t) \sin \phi_p$. Therefore, $W_p \sin \phi_p$ is made to equal W_R , thus making the two systems identical as far as the analysis is concerned. Consequently, the Bode diagram, the unity gain crossover frequency, the phase margin, and the gain margins are identical to the roll axis control system in the roll-yaw balancing mode, which is shown in FIGURE IV.

COMPUTER RESULTS

ROLL AXIS (Roll-Yaw Balancing Mode)

The simulation on the analog computer of the roll axis control system (including the dead zone and limiting characteristics) verified the linear analysis. The natural frequency of the system corresponded to the unity gain crossover frequency and the gain margins were in agreement. A response of the system to an initial unbalance torque of 200,000 dyne-cms., with $\phi_R = 90$ degrees, is shown in FIGURE VI. For variations in ϕ_R and torque (T_{UR}'), the form of the response is still the same. The chart in FIGURE VII shows the time for the total unbalance torques (T_{UR}) to reach 5,000 dyne-cms. for varying input unbalance torques (T_{UR}').

YAW AXIS (Pitch Balancing Mode)

Again the analog computer results agreed with the linear analysis. The natural frequency of the system corresponded to the unity gain crossover frequency (1 rad/sec), and the gain margins were in agreement. A response of the system to an initial unbalance torque of 200,000 dyne-cms., with $\phi_Y = 90$ degrees, is shown in FIGURE VIII, and for variations in ϕ_Y and torque input (T_{UY}'), the form of the response is still the same. The chart in FIGURE IX shows the time for the total unbalance torques (T_{UY}) to reach 5,000 dyne-cms. for varying input unbalance torques (T_{UY}').

ROLL AXIS (Pitch Balancing Mode)

First, the linearized control system was simulated on the computer, and of course the results were the same as the roll axis control in the roll-yaw balancing mode. Afterwards, the terms containing $(\cos \phi_P) \theta_R$ in equation (11), page 11, were added to see if they were negligible. No apparent change was found in the response.

A response of the system to an initial unbalance torque of 200,000 dyne-cms. is shown in FIGURE VI. The chart in FIGURE VII shows the time for the total unbalance torques (T_{UP}) to reach 5,000 dyne-cms. for varying input unbalance torques (T_{UP}'). These are the same responses for the roll axis control in the roll-yaw balancing mode.

INTER-AXIS CROSS-COUPLING

Below the general equations of angular motion of a rigid body are given from which the linear approximations

$$\Sigma T_R = I_{RR} \ddot{\theta}; \Sigma T_Y = I_{YY} \ddot{\theta}_Y \text{ result.}$$

$$(16) \quad T_R = \dot{H}_R + \omega_Y H_P - \omega_P H_Y$$

$$(17) \quad T_Y = \dot{H}_Y + \omega_P H_R - \omega_R H_P$$

$$(18) \quad T_P = \dot{H}_P + \omega_R H_Y - \omega_Y H_R$$

where:

$$H_R = I_{RR} \omega_R - I_{RY} \omega_Y - I_{RP} \omega_P$$

$$H_Y = I_{YY} \omega_Y - I_{YR} \omega_R - I_{YP} \omega_P$$

$$H_P = I_{PP} \omega_P - I_{PR} \omega_R - I_{PY} \omega_Y$$

Since the axes of the table are essentially the principal axes, the products of inertia will be much less than the moments of inertia, and therefore:

$$H_R \approx I_{RR} \omega_R ; H_Y \approx I_{YY} \omega_Y ; H_P \approx I_{PP} \omega_P$$

and

$$(19) \quad T_R = I_{RR} \dot{\omega}_R + I_{PP} \omega_Y \omega_P - I_{YY} \omega_P \omega_Y \\ = I_{RR} \dot{\omega}_R - (I_{YY} - I_{PP}) \omega_Y \omega_P$$

$$(20) \quad T_Y = I_{YY} \dot{\omega}_Y + I_{RR} \omega_R \omega_P - I_{PP} \omega_R \omega_P \\ = I_{YY} \dot{\omega}_Y - (I_{PP} - I_{RR}) \omega_P \omega_R$$

$$(21) \quad T_P = I_{PP} \dot{\omega}_P + I_{YY} \omega_Y \omega_R - I_{RR} \omega_Y \omega_R \\ = I_{PP} \dot{\omega}_P - (I_{RR} - I_{YY}) \omega_R \omega_Y$$

The maximum rates of the table when the system was simulated on a single axis basis on the computer were:

$$\omega_{RM} = 5 \times 10^{-4} \text{ RAD/SEC}$$

$$\omega_{YM} = 3 \times 10^{-4} \text{ RAD/SEC}$$

$$\omega_{PM} = 0$$

Therefore, the only important cross-coupling term would be that in equation (21), namely, $(I_{RR} - I_{YY}) \dot{W}_R \dot{W}_Y$. Since $I_{RR} - I_{YY} = 23 \text{ slug-ft}^2$, the maximum value of this cross-coupling term would be as follows.

$$(I_{RR} - I_{YY}) \dot{W}_R \dot{W}_Y = 46.5 \text{ dyne-cms.} \\ \text{or } 3.45 \times 10^{-6} \text{ ft-lb}$$

This would produce a negligible maximum acceleration about the pitch axis as can be seen by substituting this value of maximum cross-coupling torque into equation (21). The resulting $(\dot{\omega}_P)_{\text{MAX}}$ would be as follows.

$$(\dot{\omega}_P)_{\text{MAX}} = \frac{3.45 \times 10^{-6} \text{ ft-lb}}{50 \text{ slug-ft}^2} = 6.9 \times 10^{-8} \text{ rad/sec}^2$$

Since the computer results show that the balancing system always stabilizes in less than 2 minutes, the resulting velocity about pitch must be less than $6.9 \times 10^{-8} \text{ rad/sec}^2 \times 120 \text{ sec}$ or $8.3 \times 10^{-6} \text{ rad/sec}$. This is two orders of magnitude less than the maximum rates in roll and yaw, and obviously causes no further cross-coupling effects.

Consequently, all cross-coupling terms in equations (19) through (21) are negligible and can be dropped. The final equations of motion therefore reduce to the following.

$$(22) \quad T_R = I_{RR} \dot{\omega}_R = I_{RR} \ddot{\theta}_R$$

$$(23) \quad T_Y = I_{YY} \dot{\omega}_Y = I_{YY} \ddot{\theta}_Y$$

$$(24) \quad T_P = I_{PP} \dot{\omega}_P = I_{PP} \ddot{\theta}_P$$

CONCLUSION

The analog computer results show the balancing systems to be stable, and the parameters of each system should be those stated in the block diagrams (FIGURE III).

A balancing time of two minutes in each position should be a sufficient amount of time to allow the table to balance itself, and since three balancing procedures are necessary, the total time for fine balancing will be approximately 10 minutes.

APPENDIX

Since the possibility does exist to have the output shaft at right angles to the armature shaft of the motor, the torque caused by the moving armature may be used to help balance its own axis. In accordance, a very interesting result occurs. The equations of this phenomena are shown below:

$$(25) \theta_M(S) = \frac{K_M}{S(\tau_M S + 1)} E_M(S)$$

but:

$$(26) S^2 \theta_M(S) = \alpha_M(S) \quad (\text{SINCE ALL INITIAL CONDITIONS ARE ZERO})$$

and:

$$(27) T_{AM}(S) = I_M \alpha_M(S)$$

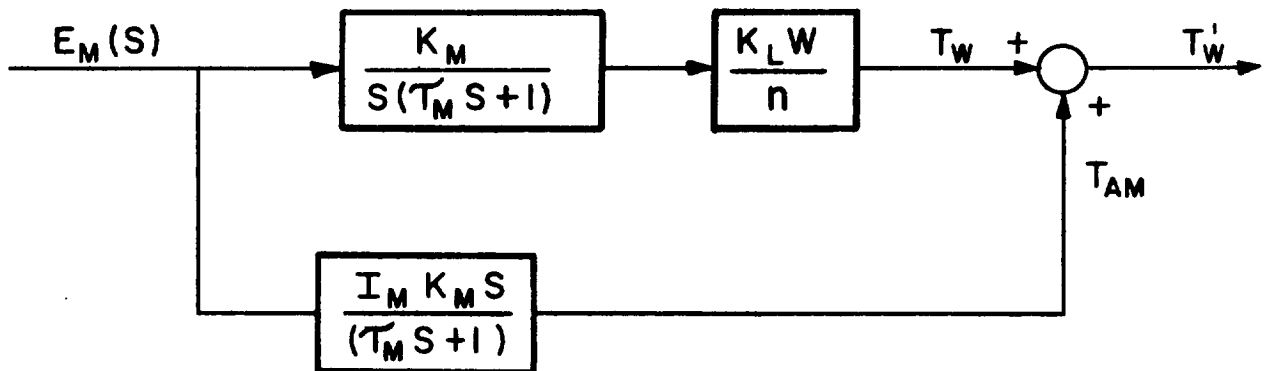
therefore:

$$(28) \alpha_M(S) = \frac{SK_M}{(\tau_M S + 1)} E_M(S)$$

and:

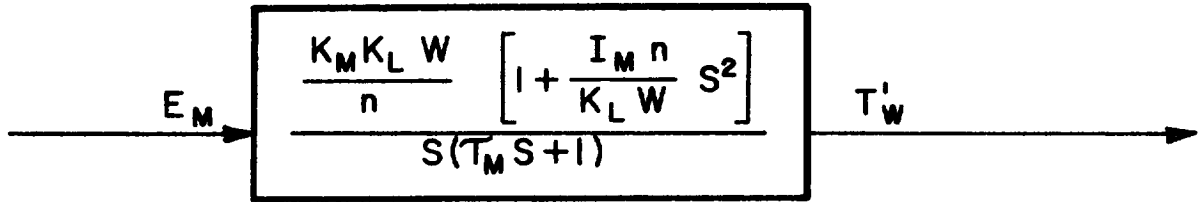
$$(29) T_{AM}(S) = \frac{I_M K_M S}{(\tau_M S + 1)} E_M(S)$$

The block diagram from the input of the motor to the torque on the table is:

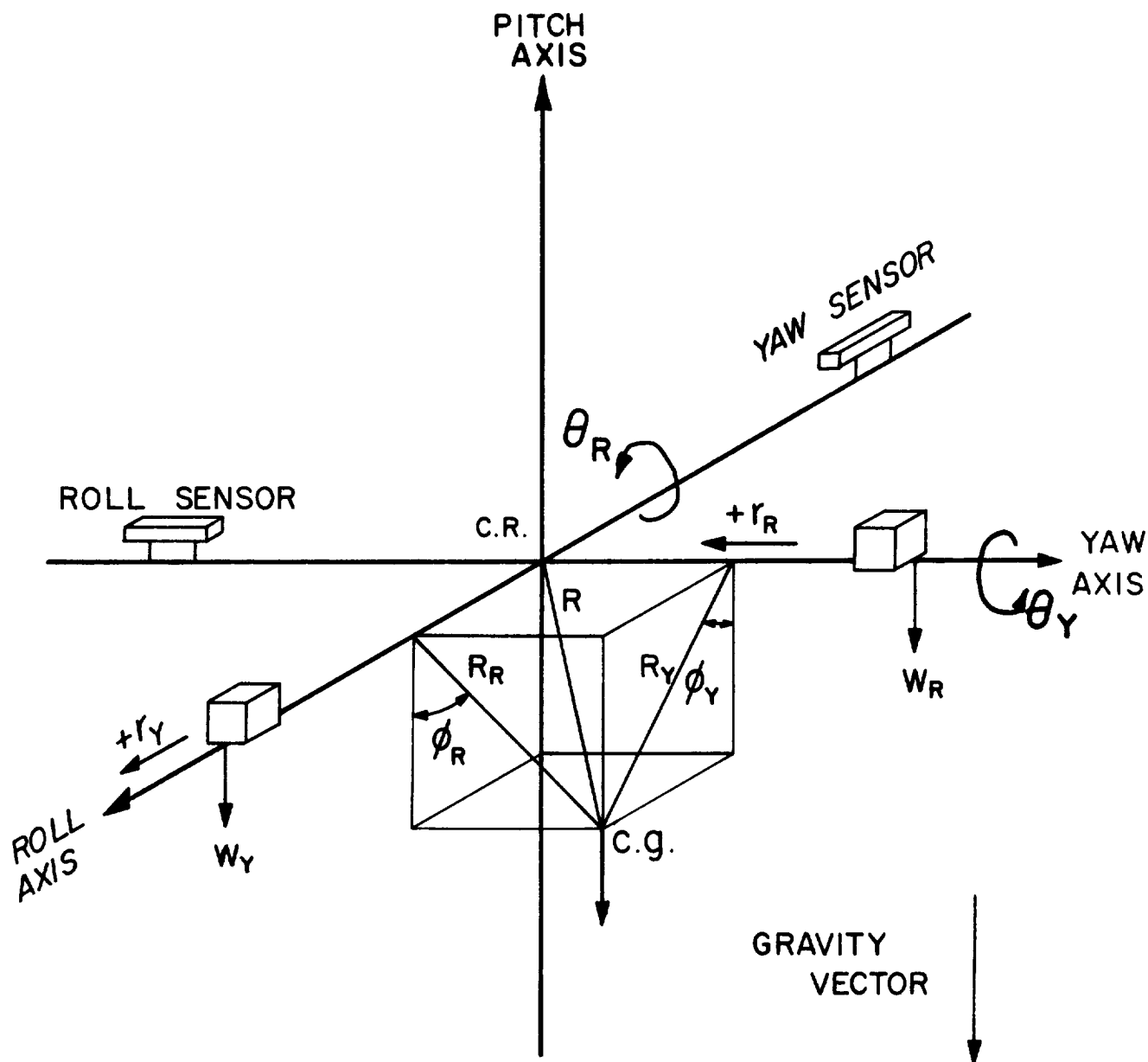


And simplifying this block diagram so that the motor, screw lead, and control weight may be represented by one block:

$$\begin{aligned}
 (30) \quad \frac{T'_W(S)}{E_M(S)} &= \frac{K_M K_L \frac{W}{n}}{S(\tau_M S + 1)} + \frac{I_M K_M S}{(\tau_M S + 1)} \\
 &= \frac{K_M K_L \frac{W}{n} + I_M K_M S^2}{S(\tau_M S + 1)} \\
 &= \frac{K_M K_L \frac{W}{n} \left[1 + \frac{I_M n}{K_L W} S^2 \right]}{S(\tau_M S + 1)}
 \end{aligned}$$

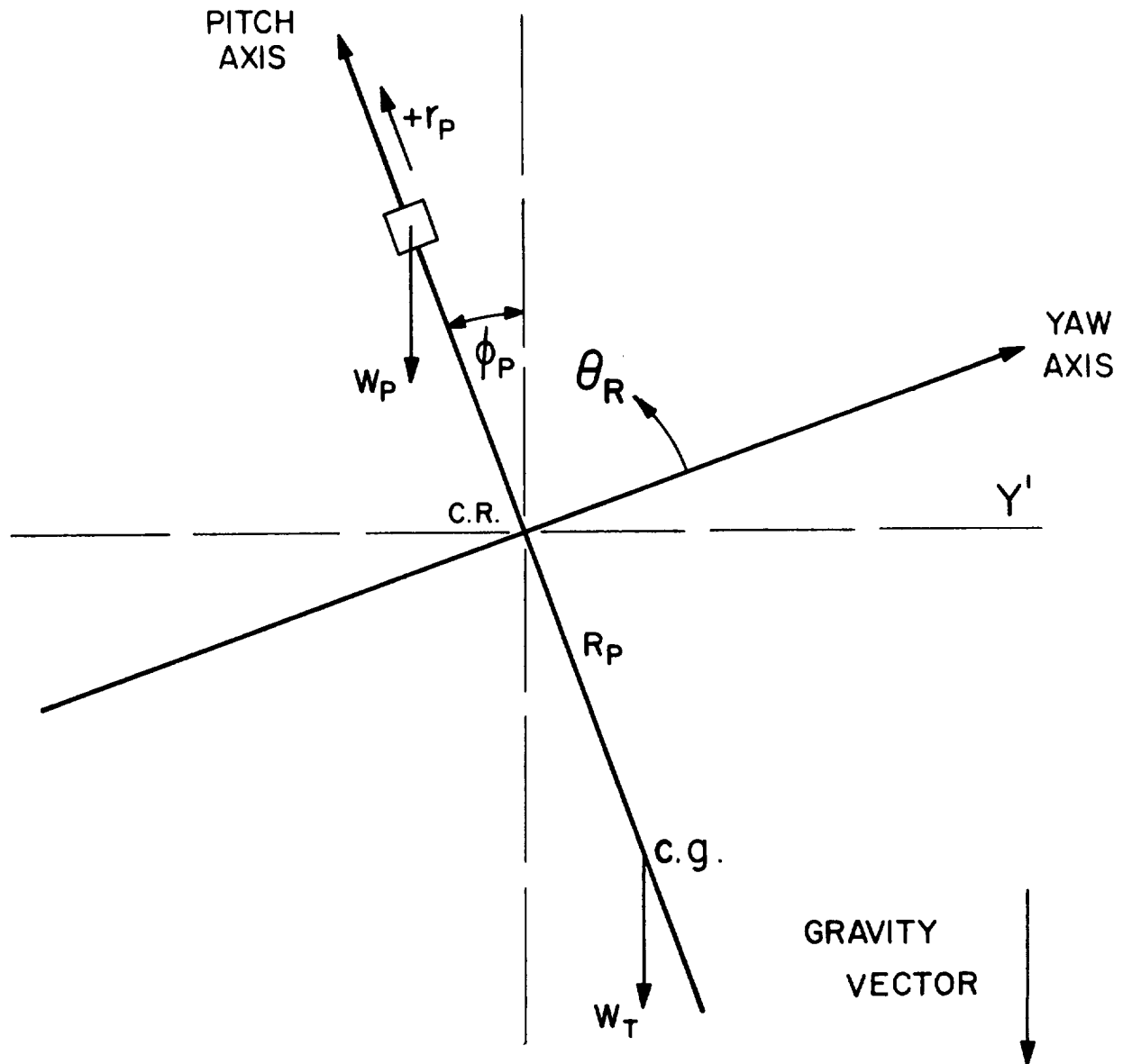


Notice that this transfer function has the lead term $(1 + I_M n s^2 / K_L W)$ in the numerator. If $I_M n / K_L W$ could be made large enough, the necessary phase lead would be obtained without any additional lead networks. However, in this system $I_M n / K_L W$ is approximately 0.2 (seconds)^2 , producing no appreciable lead in the system in the region of interest. To increase $I_M n / K_L W$ without decreasing the gain of the system, only I_M can be increased. Preliminary investigations of a motor that satisfies all the necessary conditions (a high inertia, a low starting voltage, a low operating current, and a linear, high gain, speed-voltage characteristic) show this method to be impractical for this control system. But when all the above conditions do not have to be met, and when a great amount of phase lead is necessary, this type of compensation should be considered.



ROLL-YAW BALANCING MODE

FIGURE I



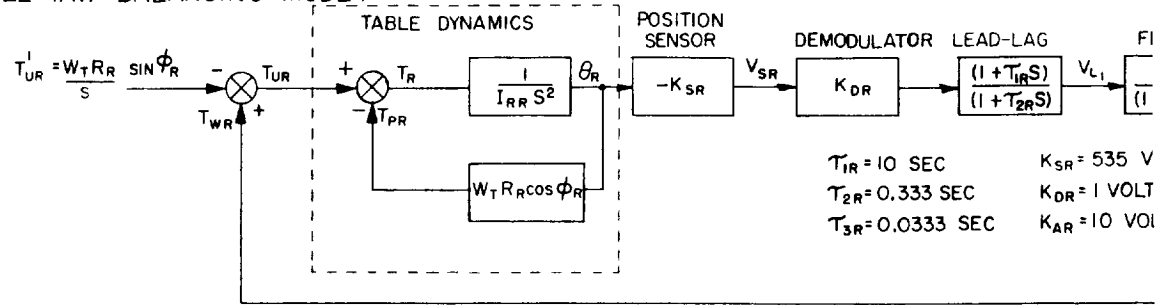
NOTE: I. THE ROLL AXIS IS POSITIVE OUT OF THE PLANE OF THE PAPER.

PITCH BALANCING MODE

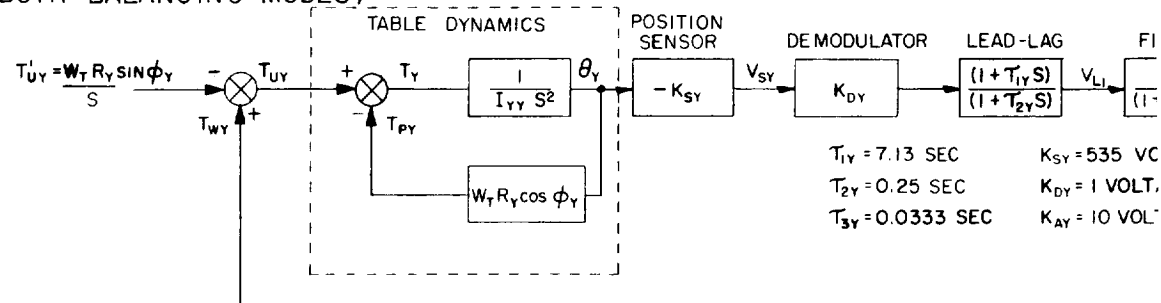
FIGURE II

2

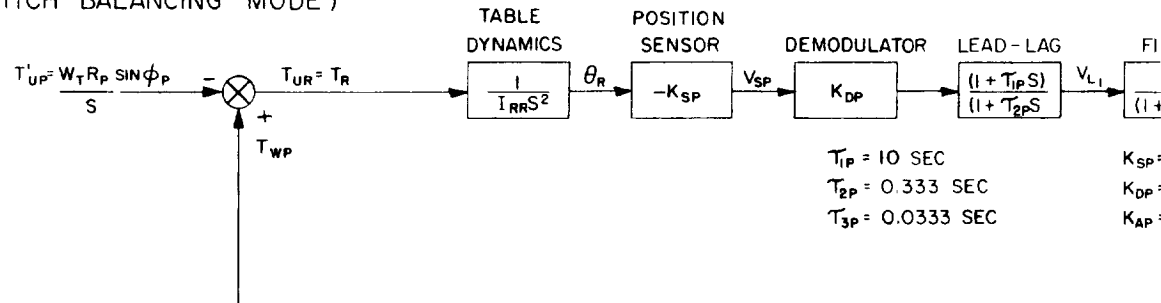
ROLL AXIS CONTROL (ROLL-YAW BALANCING MODE)



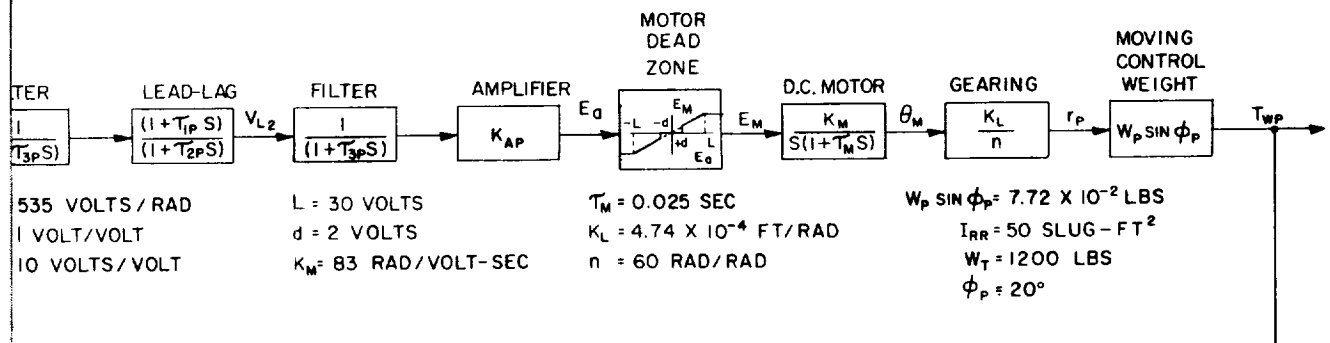
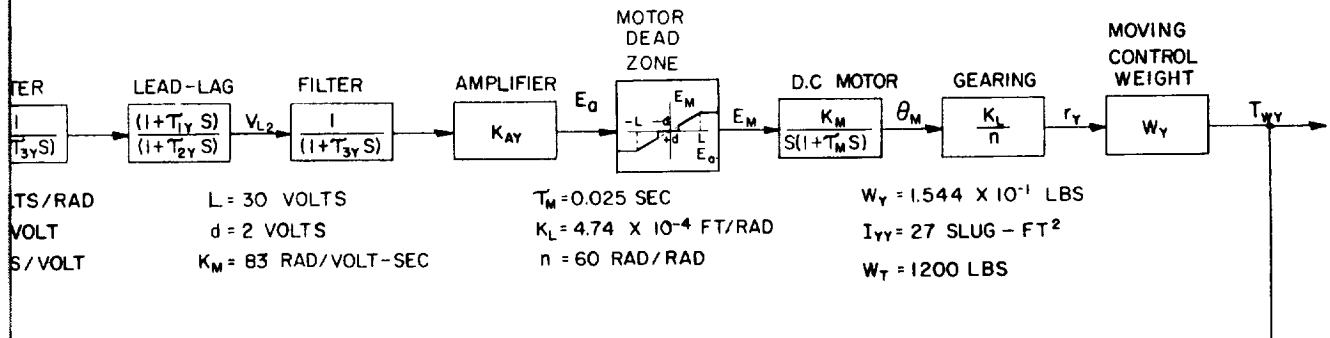
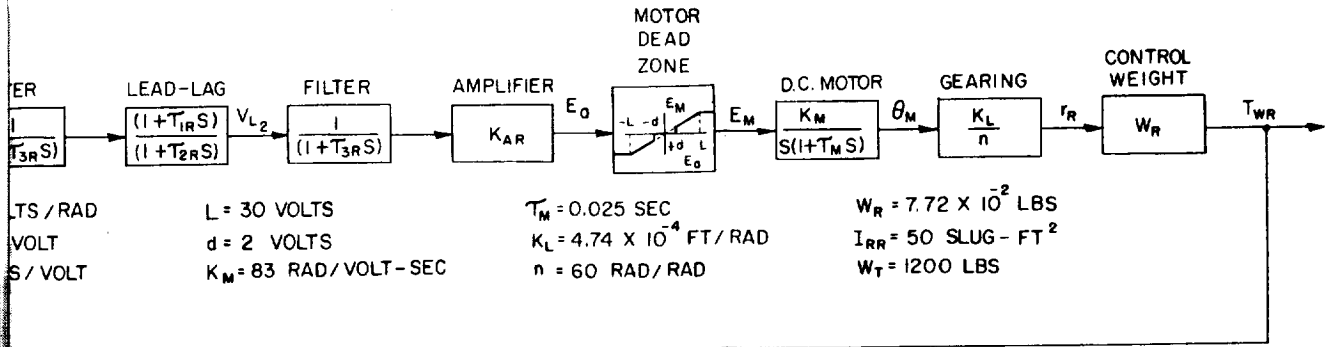
YAW AXIS CONTROL (BOTH BALANCING MODES)



ROLL AXIS CONTROL (PITCH BALANCING MODE)



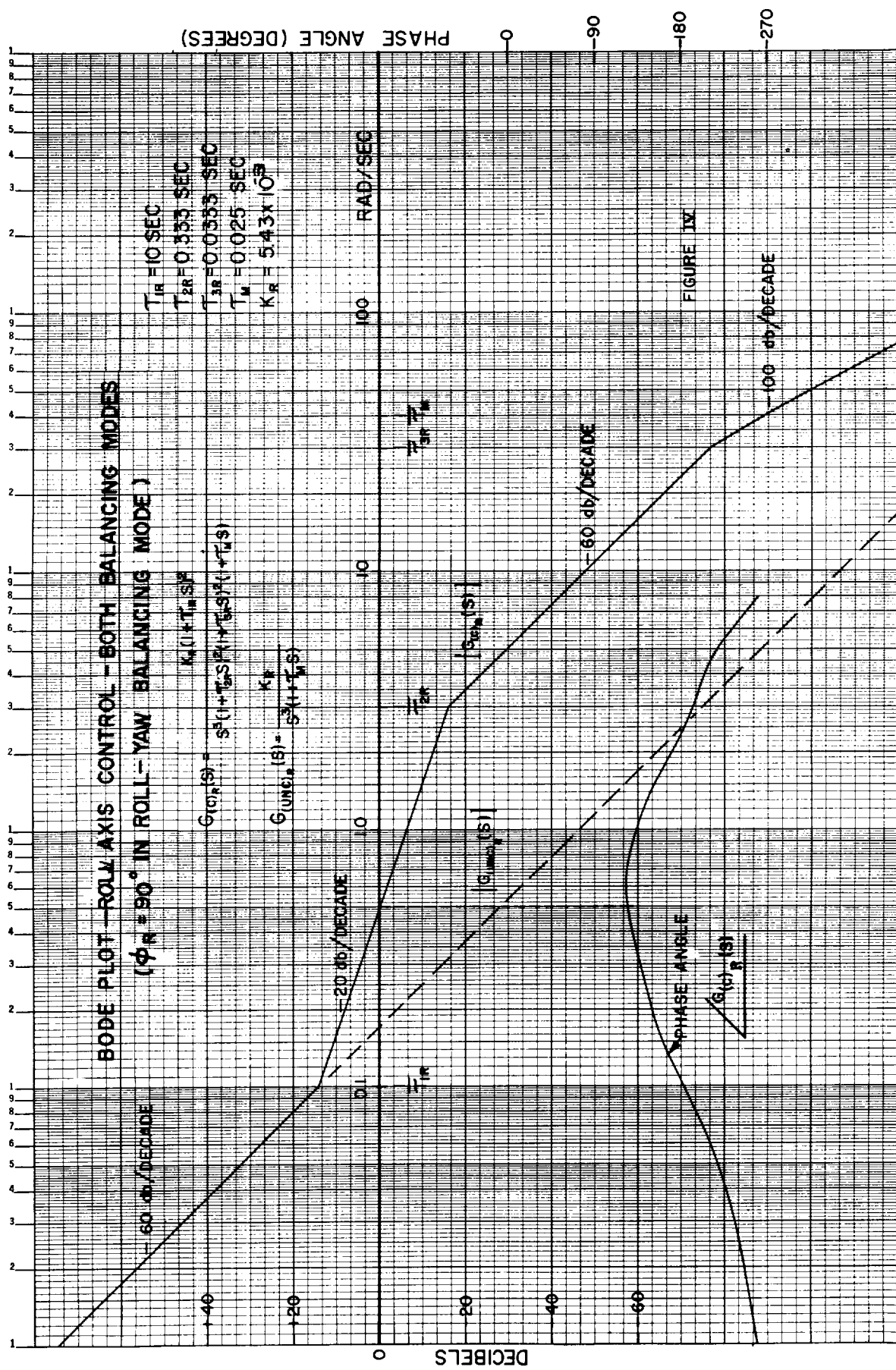
b

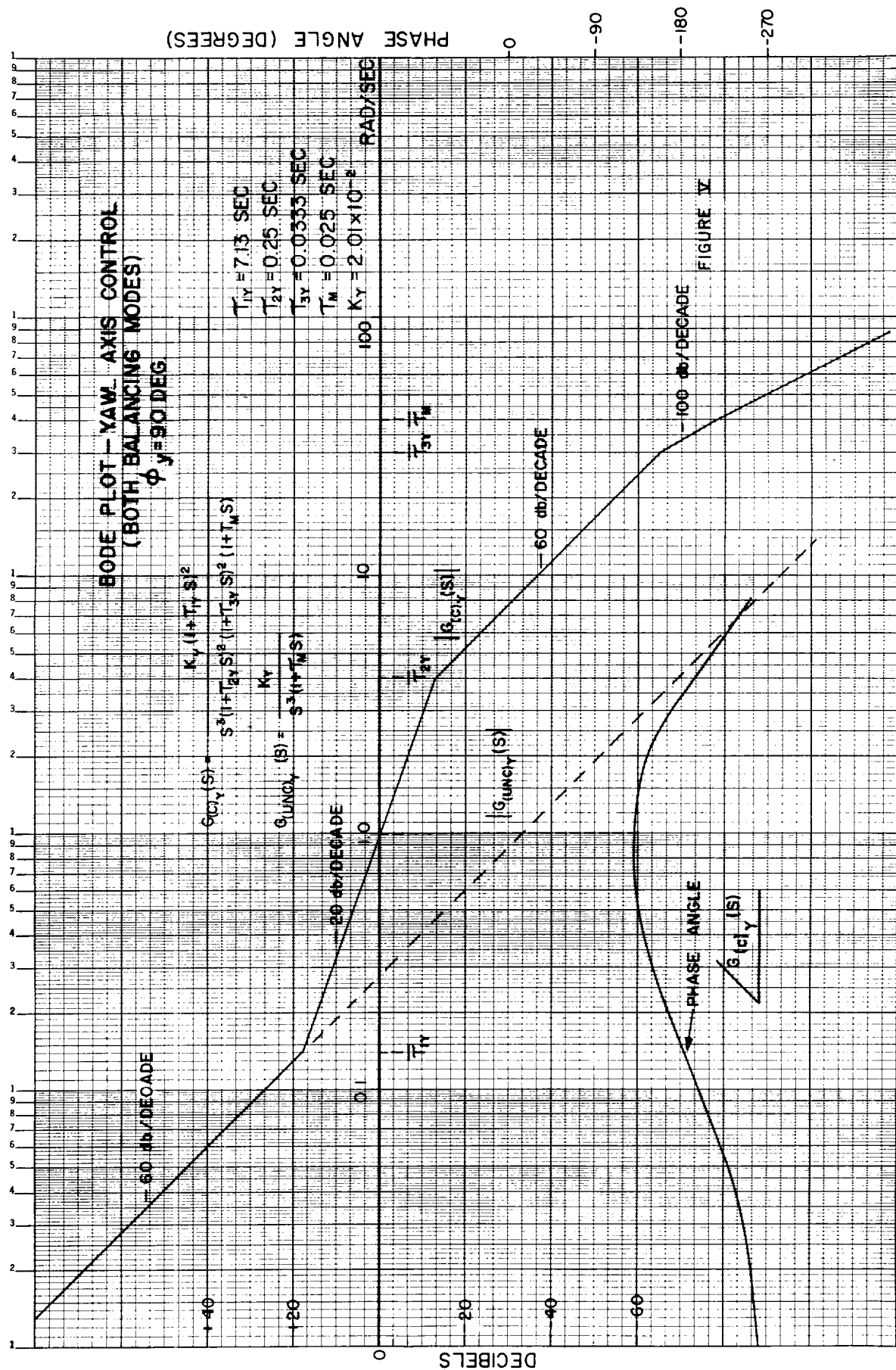


GD-SSI-1102365

FIGURE III

REV	DATE	DESCRIPTION	BY	DATE
LIST OF MATERIAL				
DESIGNED		NAME	DATE	
DRAWN		NAME	DATE	
CHECKED		NAME	DATE	
APPROVED		NAME	DATE	
BALANCING SYSTEM FOR 3 AXIS AIR BEARING TABLE SERVO BLOCK DIAGRAM				
NATIONAL AERONAUTICS AND SPACE ADMINISTRATION GODDARD SPACE FLIGHT CENTER GREENBELT, MARYLAND				
GD-SSI-1102365				





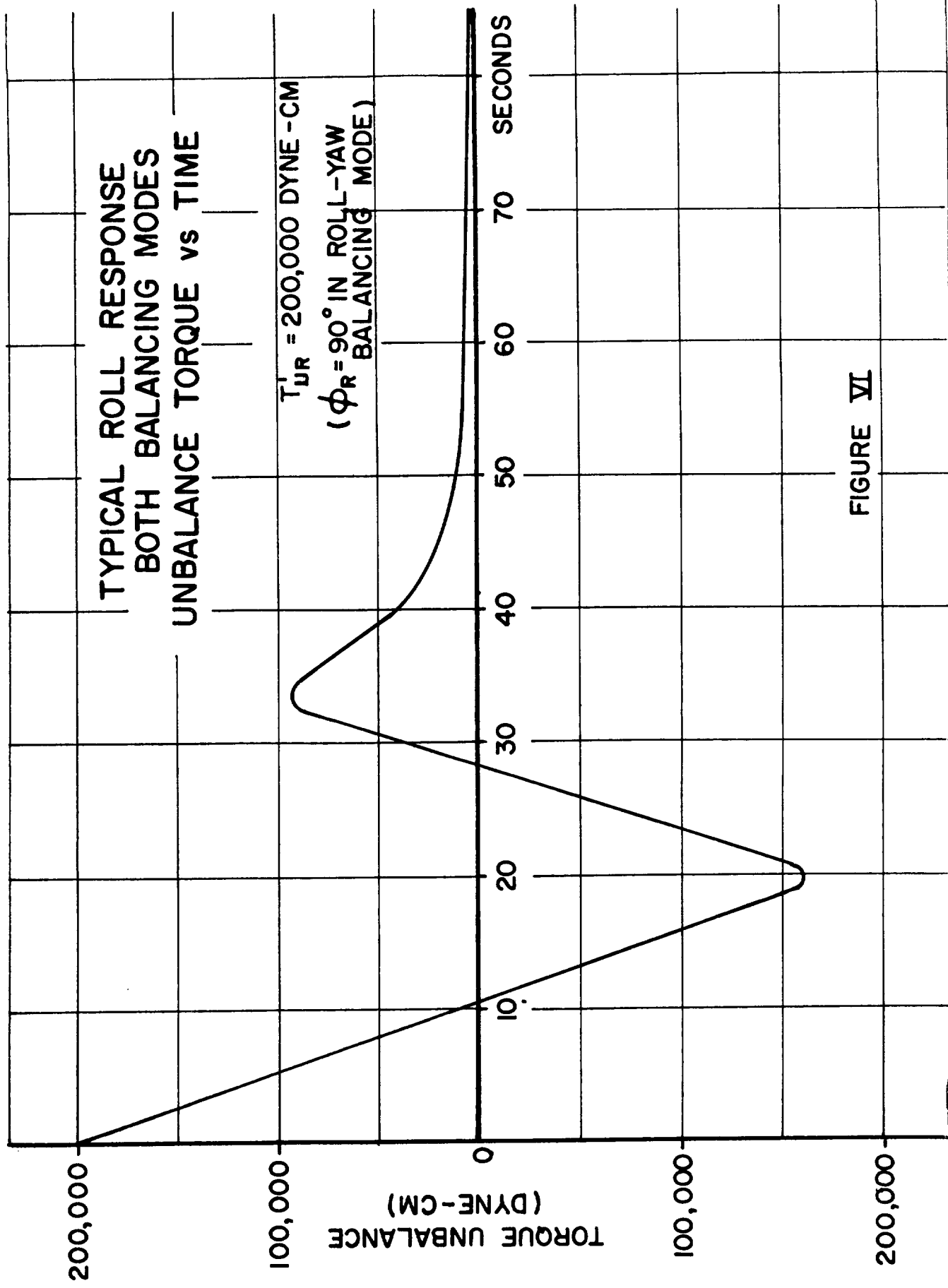


FIGURE VI

ROLL AXIS CONTROL-BOTH BALANCING MODES
($\phi_R = 90^\circ$ in roll-yaw balancing mode)

Initial Unbalance Torque vs. Settling Time to 5,000 Dyne-Cms. Balance

Torque (Dyne-Cm.)	Time (seconds)
10,000	12
20,000	13
30,000	13
40,000	13
50,000	14
60,000	14
70,000	14
80,000	15
90,000	16
100,000	45
110,000	47
120,000	50
130,000	53
140,000	56
150,000	60
160,000	65
170,000	73
180,000	80
190,000	80
200,000	80

FIGURE VII

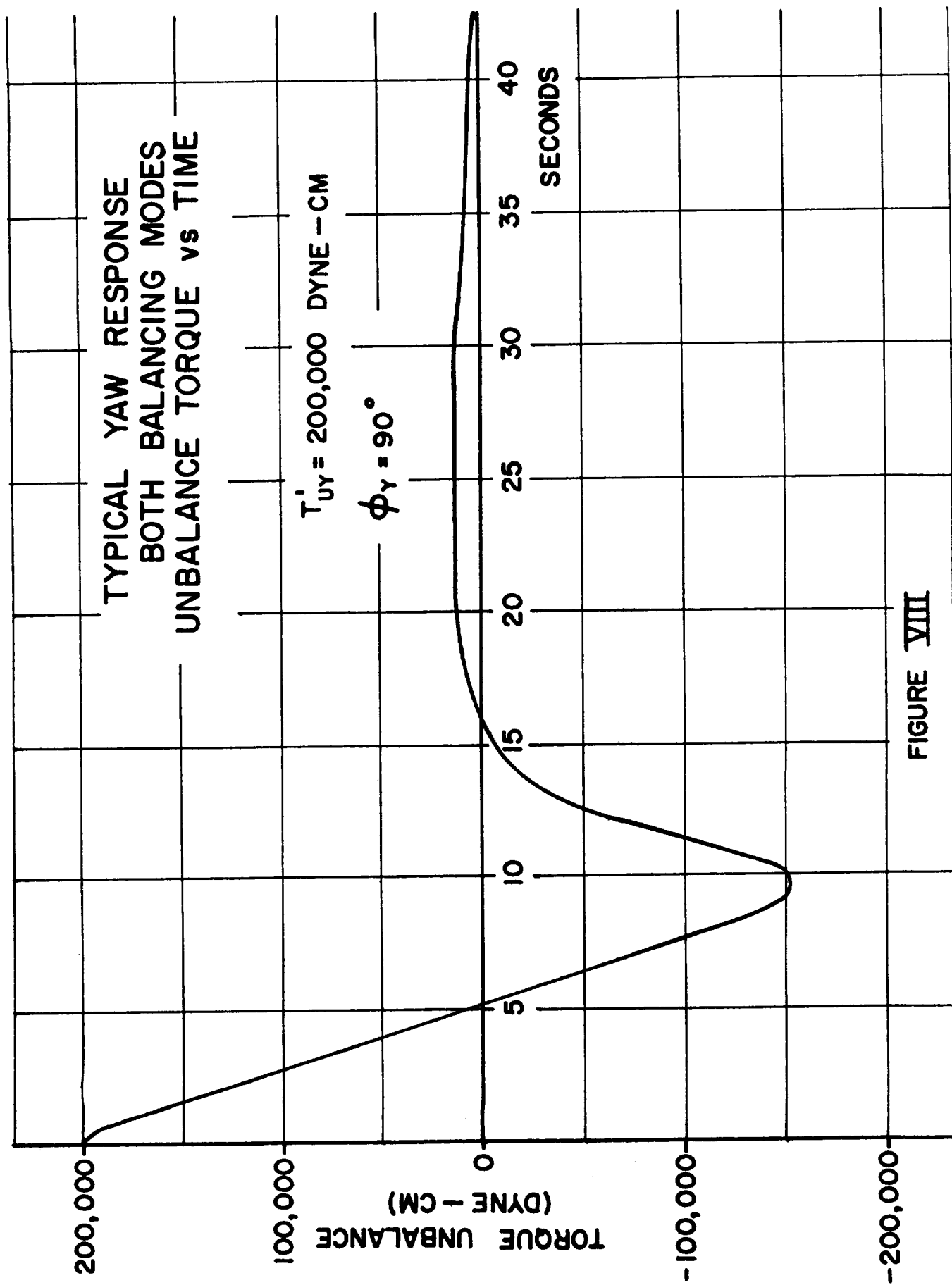


FIGURE VIII

YAW AXIS CONTROL-BOTH BALANCING MODES
($\phi_Y = 90^\circ$)

Initial Unbalance Torque vs. Settling Time to 5,000 Dyne-Cms. Balance

Torque (Dyne-Cm.)	Time (second)
10,000	2
20,000	4
30,000	5
40,000	6
50,000	8
60,000	8
70,000	9
80,000	9.5
90,000	10
100,000	11
110,000	11.5
120,000	12
130,000	13
140,000	33
150,000	34
160,000	35
170,000	35
180,000	36
190,000	37
200,000	38

FIGURE IX

